DOI: 10.1002/chem.201103256

Design, Synthesis, and Miniemulsion Polymerization of New Phosphonate Surfmers and Application Studies of the Resulting Nanoparticles as Model Systems for Biomimetic Mineralization and Cellular Uptake

Rüdiger Sauer,[a] Pablo Froimowicz,*[a] Katrin Schöller,[a] Jens-M. Cramer,[a] Sandra Ritz,[a] Volker Mailänder,[a, b] and Katharina Landfester*[a]

Abstract: Heterophase polymerizations have gained increasing attention in the past decades, especially as the decoration and functionalization of the particle surface for further applications gets more and more into focus. One promising approach for the functionalization exclusively on the particle surface is the use of surfmers (surfactant and monomer). Herein, we present the synthesis of a new family of surfmers and their use for decorating nanoparticles with phosphonate groups through miniemulsion polymerization. Furthermore the synthesis of a dye-labeled functional surfmer provided an elegant manner to evaluate and get deeper insights about its copolymerization. Additionally, potential applications of the synthesized particles in biological studies as well as their use as template for biomimetic mineralization are presented.

Keywords: biomimetic mineralization · cell uptake · miniemulsion polymerization · nanoparticles · surfmer

Introduction

The synthesis of tailored surface-functionalized nanoparticles is increasingly attracting the attention of researchers due to the vast variety of applications in which they are applied in different fields,[1] such as generation and exploitation of inorganic-organic hybrid nanomaterials through mineralization of organic templates[2] or coating the inorganic moiety with organic layer(s);[3] in biological[4] and medical researches[5] for cell uptake,[3a] or drug release,[6] and in polymers and materials sciences for studying stimuli-responsiveness.[7] However, one of the major challenges in the generation of these surface-functionalized nanoparticles is how to address an adequate organization of the matter to introduce the desired functionalities at the required location already during their preparation, thus avoiding post-polymerization chemical modifications and/or unnecessary purification steps. In this paper we show that with the use of new synthetic surfmers (one class of reactive surfactants), we were able to synthesize well defined surface-functionalized nanoparticles without the need for any further chemical post-functionalization and working under surfactant-free conditions. The resulting latexes were subsequently demonstrated to be highly applicable as a model system for different studies, as templates for biomimetic mineralization, and cell-uptake experiments.

As aforementioned, among the different kinds of reactive surfactants we decided to exploit the chemistry of surfmers because they are amphiphilic compounds behaving simultaneously as a surfactant and a co-monomer. Etymologically, the term "surfmer" is an acronym formed from the words surfactant (surface-active agent) and monomer. Thus, as any other surfactant, surfmers play a crucial role in heterophase polymerizations such as emulsion and miniemulsion polymerizations. Although these two heterophase polymerization techniques have many similarities (including compartmentalization),[8] their particle nucleation mechanisms are different. Whereas in emulsion polymerization it is micellar nucleation that dominates,[9,10] in miniemulsion polymerization the particle nucleation occurs in the stabilized monomer droplets.[8b,11,12] Thus, the role of the surfactant during the polymerization process is different for each technique, but once the polymerization is finished, surfactants are, in both cases, responsible for keeping the synthesized nanoparticles stable in the continuous phase. It is known that conventional surfactants are physically adsorbed on the polymer particles and may migrate inward or desorb from the product causing their destabilization.[12,13] To avoid these negative features of conventional surfactants, surfmers (among other reactive surfactants) have attracted increasing attention.[14,15,16] These reactive surfactants participate in the poly-

[a] R. Sauer, Dr. P. Froimowicz, K. Schöller, J.-M. Cramer, Dr. S. Ritz, Dr. V. Mailänder, Prof. Dr. K. Landfester
Max Planck Institute for Polymer Research
Ackermannweg 10, 55128 Mainz (Germany)
Fax: (+49) 6131-379-370
E-mail: landfester@mpip-mainz.mpg.de
froimowicz@mpip-mainz.mpg.de

[b] Dr. V. Mailänder
III. Medical Clinic (Hematology, Oncology, and Pulmology)
University Medicine of the Johannes-Gutenberg University Mainz
Langenbeckstr. 1, 55131 Mainz (Germany)

Supporting information for this article is available on the WWW under http://dx.doi.org/10.1002/chem.201103256.

 © 2012 Wiley-VCH Verlag GmbH & Co. KGaA, Weinheim

merization process and become constituents of the polymer backbone; therefore, they are not physically adsorbed but covalently attached to the surfaces of the polymer particles,[12] making any migration nor desorption of the surfmers no longer possible.

A distinctive characteristic of miniemulsion polymerizations is that, unlike emulsion polymerizations, the net diffusion of compounds between individual droplets is suppressed.[1,11] This difference between the two techniques also implies that the requirements on the surfmer reactivity are different. A surfmer that can be used in emulsion polymerization should have a low reactivity compared with the other monomer(s), thus being incorporated at the final stages of the polymerization.[17] This situation is important to avoid the burial of the surfmer inside the particle while this one grows during the polymerization due to the diffusion of monomers, which may affect the stability of the final product. However, a low reactivity of the surfmer would lead to a low copolymerization with the other monomer. Conversely, in miniemulsion processes the reactivity of surfmers should be high (or comparable to the one of the other monomers) to ensure their copolymerization on the surface of the nanoparticle, because they are highly likely to be at and react on the surface of the droplets, which do not change sizes during the polymerization process. Thus, the duality of acting simultaneously as surfactant and co-monomer is successfully exploited in the miniemulsion polymerization to generate surface-functionalized nanoparticles in a simple polymerization reaction without the use of high amounts of functionalized co-monomers, which would be distributed all over the particles and not strictly on their surface;[18] even if the co-monomer is too hydrophilic it could result in a homopolymerization forming a "hairy" layer around the particle,[19] affecting the particle size.

An additional benefit of the miniemulsion polymerization is that the composition of the final colloids resembles the composition of the dispersed monomer phase, thus defining each droplet as a nanoreactor. Especially with regard to copolymerization of different co-monomers and crosslinkers or embedding of dyes and drugs, this concept allows the preparation of well-defined polymeric particles, meaning that all incorporated functionalities are equally distributed in each particle.[1,11] This represents an advantageous aspect in our design because surfmers can be copolymerized by the miniemulsion process to homogeneously functionalize the nanoparticle surface.

In the cases in which surfmers contain at least one additional functional group, besides the polymerizable one, these compounds are considered as functional surfmers. They are of great interest since the introduction of tailored functionalities onto the surface of the nanoparticles (NPs) without any additional post-polymerization chemical modification is easily achieved. Those functionalities may be exploited afterward for further chemical/physical functionalization of the NPs toward specific applications. There are a few functional surfmers reported in the literature possessing alcohol,[20] carboxylic,[21] active ester,[22] sulfate,[23] phosphonate,[24,25] or phosphate,[24,25] functional groups. However, in most cases, the functional groups were not used for any further application.

Organophosphorous compounds have received increasing interest in many different research areas and applications fields, for example, biology,[5] biomedicine,[26] and technology.[27] Although most of the organophosphorous-containing polymerizable compounds known from literature, such as acrylates or methacrylates, consist of short alkyl spacers between the two functionalities (therefore viewed as conventional co-monomers), it has been established that for many scientific and technological applications, long alkyl-chain spacers are desirable.[25] These long-chain phosphorous-containing compounds may be viewed as surfactants and even as phospholipids analogues, and similar structures bearing polymerizable groups may be considered as surfmers. In this context, Francová and Kickelbick[24–25] described the synthetic pathway of a family of methacrylate-functionalized phosphonate amphiphiles containing alkyl spacers with a variable length, their micellization in aqueous media, and final polymerization to crosslink the nanospheres. The final product showed that the generated nano-objects presented a large size distribution. This inconvenience should be solved straightforwardly by using miniemulsion polymerization as an alternative for generating phosphonate-functionalized nanospheres. As aforementioned, the miniemulsion technique allows the synthesis of well-defined nanoparticles with controlled particle size and narrow size distribution by using low amounts of surfactants, which are advantageous if the particles are going to be used for coatings or biomedical applications. Recently the synthesis of surface phosphonate-functionalized styrene and methyl methacrylate nanoparticles was reported,[28] which were later used for cell uptake and adhesive coatings for titanium implant materials.[5] To this end, they used vinylphosphonic acid or vinylbenzylphosphonic acid as co-monomers in miniemulsion polymerizations and additional surfactants were required to stabilize the systems.

Similar surface phosphonate-functionalized nanoparticles were applied as templates for the biomimetic mineralization of hydroxyapatite (HAP).[18b] Once again, the desired functionalities were incorporated by miniemulsion copolymerization of phosphonic acid-containing co-monomers and additional surfactants. Phosphonate-functionalized particles are very well-suited as templates for the formation of bone mineral. For example, organic bisphosphonates are already used as physiological regulators for bone resorption in medicine because they strongly bind to HAP crystals.[29]

The previous examples show that the exploitation of phosphonate-containing surfmers would be highly beneficial to functionalize the nanoparticles surface since it implies working under surfactant-free conditions, causing less work up, and also allowing for a better control in the particle and distribution sizes.

Herein, we present the synthesis of novel phosphonate-containing polymerizable surfactants bearing a methacrylamide group as polymerizable unit and a phosphonic acid as

 © 2012 Wiley-VCH Verlag GmbH & Co. KGaA, Weinheim

polar head separated by a hydrophobic spacer, as shown in Schemes 1 and 2. The exploitation of the synthesized compounds in miniemulsion polymerizations of styrene and methacrylates is also presented. Additionally, the first ever fluorescent surfmer (Scheme 3) was synthesized and studied as a model system to evaluate the copolymerization of surfmers in miniemulsion polymerizations. Finally, application studies of the phosphonate-functionalized nanoparticles obtained using the previously synthesized surfmers were carried out to evaluate the viability and applicability of these systems. Specifically, on one hand, phosphonate-functionalized nanoparticles were successfully utilized to carry out cellular-uptake experiments. And on the other hand, we effectively performed surfmer-mediated biomimetic mineralization of HAP by using the same surface-functionalized nanoparticles as templates.

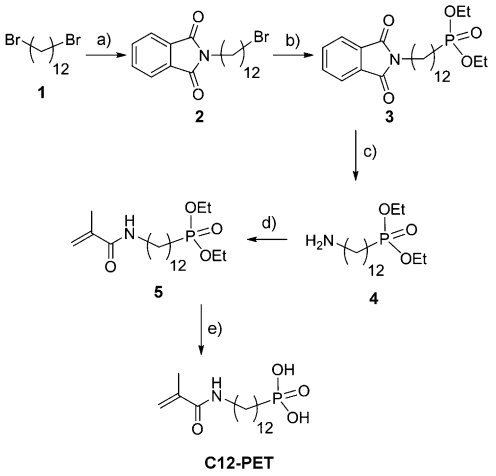

Scheme 1. Synthesis route to C12-PET. a) phthalimide potassium salt, DMF, 16 h at 80 °C; b) triethyl phosphite, 16 h reflux; c) hydrazine monohydrate, EtOH, 30 min at 0 °C, 2.5 h reflux; d) methacryloyl chloride, H_2O, CH_2Cl_2, Na_2CO_3, 30 min at 0 °C, 3 h at RT; e) i) TMSBr, CH_2Cl_2, 3 h at RT; ii) MeOH, 3 h at RT.

Results and Discussion

Synthesis of the surfmers: *Synthesis of C12-PET*: To functionalize a particle exclusively on the surface with phosphonate groups in a miniemulsion approach, a compound that bears a polymerizable group and has a hydrophobic tail of the appropriate length to balance the hydrophilicity of the headgroup is needed. Taking the hydrophilic-lipophilic balance (HLB) theory into account a spacer with 12 -CH_2- units seemed to be the best choice to balance a phosphonate headgroup. Also different authors have reported the high surface activity of dodecylphosphonic acid and tetradecylphosphonic acid.[30]

It has been reported that the position of the polymerizable group in the molecule has a great influence on the copolymerization of the compound in an emulsion/miniemulsion polymerization process.[31] As a general rule, we consider that it is more appropriate to locate the polymerizable group at the very end of the hydrophobic segment because it may be deeply immersed into the (hydrophobic) monomer phase. We designed the incorporation of the polymerizable moiety by an amide linkage, forming a methacrylamide. The synthetic strategy was tailored in such a way that no additional steps for protection–deprotection of functional groups were needed, and the sensitive polymerizable group could be incorporated in one of the last steps, as shown in Scheme 1.

12-Methacrylamidododecylphosphonic acid (**C12-PET**) was synthesized starting from 1,12-dibromododecane, which is an inexpensive compound and commercially accessible for large scale synthesis.

To obtain compound **4** a combination of the Gabriel synthesis with the Arbuzov reaction was designed. First, compound **1** was asymmetrically monosubstituted using potassium phthalimide by using the first step of the Gabriel synthesis. The phthalimide group was used as a protecting group of the already incorporated primary amine in compound **2**, which permitted us to perform the Arbuzov reaction to incorporate a phosphonic ester at the other end of the hydrocarbonated chain. Triethylphosphite ($P(OEt)_3$) was used as reagent and solvent, giving phosphonate **3** in excellent yield. Among the different possibilities for the cleavage of the phthalimide group, we considered that it is more convenient to carry it out using hydrazine, what is also known as the Ing–Manske variation of the Gabriel synthesis.[32] Thus, we deprotected the amine group in compound **3** generating **4**.

Amidation of compound **4** was performed with methacryloyl chloride to give compound **5** under Schotten–Baumann conditions. Thus, the amidation was performed as a heterophase reaction under basic conditions. The great benefit of this heterophase reaction, consisting of dichloromethane and water, is that an inorganic base could be used, which is only soluble in water and therefore easy to remove once the reaction is finished.

Deprotection of the phosphonic acid to finally generate **C12-PET** was achieved by applying a modified method from the one previously reported by McKenna and co-workers.[33] In the first step a transesterification of the phosphonic acid ester to the trimethylsilyl phosphonate is realized, by treating the ester with an excess of bromotrimethylsilane (TMSBr). In contrast to the McKenna route, which consists in using water for cleaving the freshly formed trimethylsilyl phosphonate, methanolysis was our choice.

*Synthesis of **C11-PET***: As predicted by the HLB-theory **C12-PET** exhibited remarkably good properties in miniemulsions, as will be shown later in the miniemulsion polymerization section. However, the synthetic pathway only enabled very low yields of **C12-PET** to be obtained. Based on these two facts, we designed a new synthetic approach, in which the improvements were made on the first steps of the synthesis. To synthesize **C12-PET**, the first step involved the generation of an asymmetric compound, which led to a very low yield of compound **2**; this step is now replaced by the

 © 2012 Wiley-VCH Verlag GmbH & Co. KGaA, Weinheim

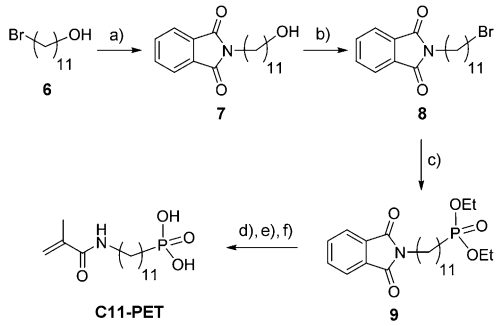

Scheme 2. Synthesis of **C11-PET**. a) phthalimide potassium salt, DMF, 16 h at 80 °C; b) PBr_3, toluene, 2.5 h at 100 °C; c) triethyl phosphite, 16 h reflux; d) hydrazine monohydrate, EtOH, 30 min at 0 °C, 2.5 h reflux; e) methacryloyl chloride, H_2O, CH_2Cl_2, Na_2CO_3, 30 min at 0 °C, 3 h at RT; f) i) TMSBr, CH_2Cl_2, 3 h at RT; ii) MeOH, 3 h at RT.

two step synthesis of compound **8** (Scheme 2), which can be considered as a synthetic equivalent of compound **2** because the compounds only differ in one -CH_2- unit. Even though the new synthetic pathway included one more step, the procedures for synthesizing and purifying the compound were much simpler and efficient, enabling a much higher overall yield for compound **8** (61%) than for **2** (15%). The new generated surfmer (**C11-PET**) would have a hydrophobic spacer formed by a -$(CH_2)_{11}$- unit, which is expected not to significantly change the properties exhibited by **C12-PET** since the only difference between both compound is just one -CH_2- unit.

Specifically, substitution of the bromine in compound **6** by phthalimide and subsequent bromination of the alcohol of the freshly obtained compound **7** by using phosphorus tribromide (PBr_3) gave the designed product **8**. Both products **7** and **8** were purified by recrystallization. From this point on, all the following steps in the synthesis of surfmer **C11-PET** were carried out as already described for **C12-PET**. As a result of the new synthetic design the overall yield for **C12-PET** (7%) was remarkably enhanced in the synthesis of **C11-PET** (36%). Moreover, **C11-PET** was also subjected to miniemulsion polymerizations showing no significant differences with **C12-PET**, as will be shown and discussed in the miniemulsion polymerization section.

*Synthesis of **Fluoro-PET***: Surfmers are likely to be incorporated into the polymer backbone, however, a major challenge in this research field is how to demonstrate the covalent attachment of the surfmer to the polymeric particles. A great deal of work has been undertaken to try to evidence the copolymerization in different studies. The authors monitored the surface tension,[16,34] dialyzed the samples extensively and measured the particle charge[35] or determined the amount of surfactant in the supernatant after centrifugation by using size-exclusion chromatography (SEC) and NMR studies,[34a] or NMR spectroscopy on the latex itself by using pulse sequences for water suppression.[13,31] Other procedures included the serum replacement method and subsequent two-phase titration[36] or extensive dialysis of the samples, which were then measured by IR spectroscopy.[37] As surfactants might be strongly adsorbed onto the particle surface, which might lead to an incomplete replacement by the aforementioned methods, we have chosen another approach that gave us the opportunity to analyze and prove the covalent attachment in a more reliable manner. We synthesized a dye-containing surfmer, which could be straightforwardly studied after polymerization by SEC overlapping both the RI and UV chromatograms. The chemical structure is comparable to **C12-PET** and **C11-PET**. A fluorescent naphthalimide group was chosen as the label. The fluorogenic 4-bromo-1,8-naphthalenedicarboxylic anhydride is commercially available and could be chemically addressed straightforwardly at two different sites with high selectivity for its functionalization.[38] The synthetic approach is presented in Scheme 3.

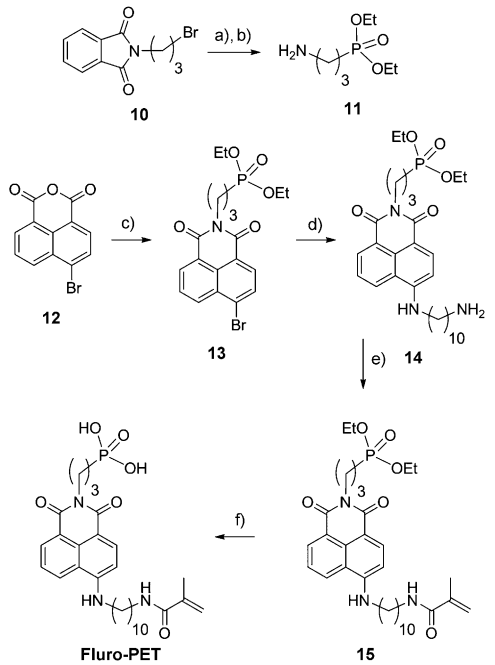

Scheme 3. Synthetic strategy for **Fluoro-PET**: Synthesis of **11**: a) triethyl phosphite, 16 h reflux; b) hydrazine monohydrate, ethanol, 30 min at 0 °C, 2.5 h reflux. Synthesis of **Fluoro-PET**: c) compound **11**, ethanol, reflux, overnight; d) diaminodecane, dioxane, triethylamine, 60 h reflux; e) methacryloyl chloride, water, CH_2Cl_2, methanol, Na_2CO_3, 30 min at 0 °C, 3 h at RT; f) i) TMSBr, DMF, overnight at RT; ii) MeOH, 3 h at RT.

The hydrophilic headgroup of the fluorescent surfmer (phosphonic acid group) is linked to the fluorogenic system by the formation of an imide bond and separated by a -$(CH_2)_3$- spacer to form the imide **13**. The anhydride group in **12** was reacted with diethyl 3-aminopropylphosphonate (**11**), which was beforehand synthesized in a two-step synthesis from the commercially available compound **10**, using the Arbuzov reaction as well as the Ing–Manske variation of the Gabriel synthesis.

 © 2012 Wiley-VCH Verlag GmbH & Co. KGaA, Weinheim

By means of a nucleophilic aromatic substitution, 1,10-diaminodecane was incorporated into the naphthalimide moiety, replacing the bromine in position 4 to generate compound **14**. The polymerizability of the molecule was again achieved by amidation of the free amine group in **14** with methacryloyl chloride under Schotten–Baumann conditions, obtaining **15** in a very good yield. In the final step, **Fluoro-PET** was synthesized by cleaving the phosphonic esters in **15** using the same procedure as for **C12-PET** and **C11-PET**. All the synthesized products were analyzed by ^{1}H, ^{13}C, ^{31}P NMR spectroscopy and mass spectrometry. Moreover, the absorption and emission spectra were recorded for the fluorescent compounds. **Fluoro-PET** was obtained as a yellow powder, which is soluble in water under slightly basic conditions. The absorption and emission spectra show only a slight overlap, with an absorption maximum at 467 nm and emission maximum at 550 nm in water, with a Stokes shift of 83 nm. As will be shown in the later sections, this compound shows the desired characteristics, including absorbance, fluorescence, polymerizability, and surface activity.

As aforementioned, compound **12** can be selectively modified at two different sites,[38] either by reacting the anhydride or substituting the bromine in position 4. The decision for the incorporation of the hydrophilic group in the fluorophore by the formation of an imide was based mainly on the final molecular geometry of the final **Fluoro-PET**, since the naphthalimide group is highly conjugated and voluminous compared with the other groups forming this surfmer and also compared with the previously synthesized **C12-PET** and **C11-PET**. Therefore, we considered it important to orientate the more polar side of the chromophore (the imide group) toward the same direction in which the headgroup (phosphonic acid) was placed, thus leading to a more realistic comparability between all the three surfmers.

Miniemulsion polymerization: The synthesized compounds were evaluated on their ability to stabilize miniemulsions. Thus, different miniemulsion systems varying monomers, ratio of surfmer and initiators were studied. The non-polymerizable surfactant sodium dodecylphosphonate (**SDP**) was used as a reference in control experiments. If not otherwise stated, in all cases the surfactant/surfmer solution used to prepare the continuous phase was 0.01 mol L^{-1}, for simplicity reasons this concentration is referred to as the standard concentration. The number in front of the surfactant/surfmer in the tables is a multiplication factor for the standard concentration, thus 2·**C12-PET** means that a solution of 0.02 mol L^{-1} was used in that particular synthesis. All miniemulsions were filtered prior to analysis to eliminate any interference from the very slight amount of coagulum present in some samples.

C12-PET *as surfmer for miniemulsion polymerization*: As predicted by the HLB theory, **C12-PET** showed to be a very effective surfmer since it was highly efficient stabilizing the miniemulsion and resulting dispersions. Results showed that increasing the ratio of **C12-PET** in the polymerizations produced diminution in the particle size of the synthesized nanoparticles. Different monomers could be polymerized. Both organic- and water-soluble initiators were demonstrated to initiate the free-radical polymerizations and the solid content after polymerizations were always very close to the theoretical values. All the results are presented in Table S1 in the Supporting Information. These results showed that **C12-PET** behaved as a surfmer rather than as a conventional co-monomer.

Figure 1 shows representative SEM images of the different latexes synthesized using **C12-PET** as surfmer. It can be seen from the pictures that all systems polymerized giving narrow size distributions. Figure 1 A and B show the change

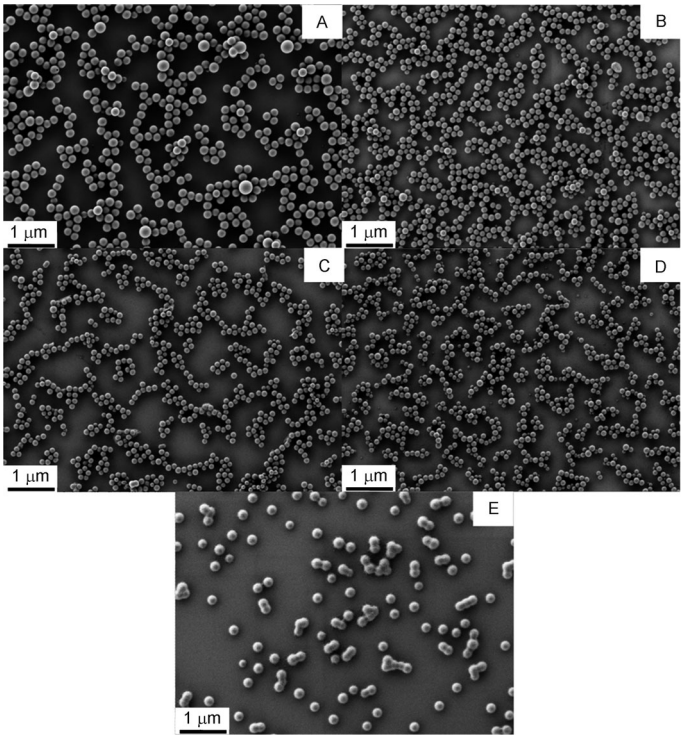

Figure 1. SEM images of nanoparticles stabilized with **C12-PET**. A) polystyrene, initiator V59, 0.5 **C12-PET**; B) polystyrene, initiator V59, 1.0 **C12-PET**; C) polystyrene, initiator KPS, 1.0 **C12-PET**; D) polystyrene, initiator KPS, 1.0 **SDP**; E) poly(*n*-butyl methacrylate), initiator KPS, 1.0 **C12-PET**. The number in front of the surfactant/surfmer is a multiplication factor for the standard concentration (0.01 mol L^{-1}).

in particle size varying the concentration of the surfmer from 5 to 10 mmol·L^{-1}, respectively, and the results were confirmed by the dynamic light scattering (DLS) measurements (see Table S1 in the Supporting Information). Both of these systems were polymerized using V59 as a hydrophobic initiator.

Figure 1 C shows a SEM image of a latex polymerized in similar conditions as for the one shown in Figure 1 B, but when using the water-soluble KPS initiator we obtained no significant characteristic differences between the systems

 © 2012 Wiley-VCH Verlag GmbH & Co. KGaA, Weinheim

(see Table S1 in the Supporting Information). For comparison, nanoparticles prepared with the conventional surfactant **SDP** and KPS are presented in Figure 1 D. Figure 1 E shows particles of poly(*n*-butyl methacrylate) (PBMA). As PBMA has a T_g slightly higher than room temperature, the particles tend to melt under the electron beam and then they do not look perfectly spherical.[39] However, it is still possible to notice the nice narrow size distribution of the resulting nanoparticles.

To study the covalently attachment of **C12-PET** to the polymer backbone additional studies were carried out. We designed a series of complementary NMR experiments to study the presence or absence of the polymerizable methacrylamide belonging to **C12-PET** by studying the proton spectra of the methacrylamide by ^{1}H NMR spectroscopy ($H_2C{=}C(CH_3)$-). The results are presented in Figure 2 A.

To evaluate the polymerization of the surfmer three samples were prepared and studied by ^{1}H NMR spectroscopy: pure surfmer **C12-PET** (spectrum i); as a reference a polystyrene dispersion polymerized using **SDP** (see **PS-1** in the Supporting Information) was dialyzed, then 1 mL was freeze-dried and the initial amount of **C12-PET** (as for **PS-2**) was added, finally the mixture was re-suspended in 1 mL [D$_6$]DMSO (spectrum ii); 1 mL of a freshly prepared polystyrene dispersion polymerized using **C12-PET** (**PS-2** in the Supporting Information) was freeze-dried and re-suspended in 1.0 mL [D$_6$]DMSO (spectrum iii). Spectrum iii in Figure 1 A shows that the signals from the methacrylamide protons belonging to the surfmer were not detectable for the polymerized surfmer, whereas in the case of the mixture (spectrum ii), used as reference, the signals of those protons were clearly visible at $\delta = 5.6$ and 5.3 ppm and are in good accordance with the chemical shifts for the protons of the surfmer, as evidenced by spectrum i, which corresponds to pure **C12-PET**.

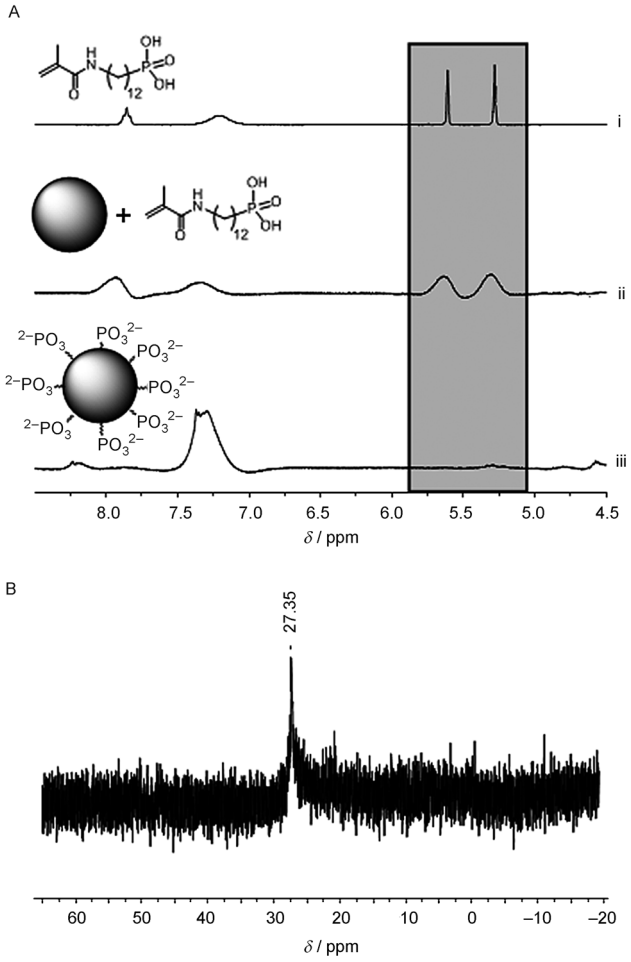

Figure 2. A) ^{1}H NMR spectra sections in [D$_6$]DMSO: i) **C12-PET**, ii) dispersion stabilized with **SDP** and **C12-PET** added (**PS-1**), iii) dispersion stabilized with **C12-PET** (**PS-2**). B) ^{31}P NMR of **PS-2**, dialyzed, freeze-dried and redispersed in [D$_6$]DMSO.

A complementary control experiment to test the sensitivity of the previous NMR measurements was carried out by performing ^{31}P NMR analysis of the polymerized sample in which **C12-PET** was used. To this end, we used the same sample studied by ^{1}H NMR spectroscopy and shown in Figure 2 A, spectrum iii; the result is presented in Figure 2 B. It can be seen that the signal at $\delta = 27.35$ ppm belonging to the phosphonate groups is clearly observable. The fact that this signal is broadened shows that the phosphonates have a limited mobility caused by their covalent attachment to the particle surface. Thus, the complementary information collected upon ^{1}H and ^{31}P NMR measurements shows that a) the surfmer can be easily detected and is highly possible that is located on (or at least near) the surface of the particle; and b) whereas the phosphonates indicate their presence on the particle surface, the absence of the proton signals belonging to the polymerizable moiety strongly suggest that this has been copolymerized forming part of the nanoparticle polymer backbone.

C11-PET and Fluoro-PET as surfmers for miniemulsion polymerization: To study the influence in particle sizes and to determine where the amount of surfactant is no longer sufficient for the stabilization of the miniemulsions, a series of miniemulsions were synthesized by using **C11-PET** and **Fluoro-PET** with decreasing amounts of surfmer. As a measure for the stability and efficiency of the surfmer, the solid content after filtration and a monomodal particle size distribution were taken into account. The results are summarized in Table 1 for **C11-PET** and Table 2 for **Fluoro-PET**.

As shown in the two tables, the **Fluoro-PET** miniemulsions seem to be more stable in this concentration range since in the case of **C11-PET** the solid content is decreasing when the surfmer amount is lowered under a certain level. As can be seen from Table 1 and Table 2, the particle size depends on the amount of surfmer used; the higher the amount of surfmer, the smaller the particle sizes.

In addition, the hydrophilicity of the monomer seems to affect the final particle size; thus, with the same amount of surfmer, the particles are bigger for both **C11-PET** and **Fluoro-PET** when using methyl methacrylate than for those obtained using styrene.

© 2012 Wiley-VCH Verlag GmbH & Co. KGaA, Weinheim

Table 1. Concentration series of **C11-PET** for stability test, for styrene and methyl methacrylate polymerizations.

Samples[a]	Monomer	Surf. ratio	DLS		Solid content [%]
			d_h [nm]	σ [nm]	
PS-1s	St	2.0	140	19	21.5
PS-2s	St	1.0	204	23	19.7
PS-3s	St	0.5	280	30	14.7
PS-4s	St	0.25	315	37	12.2
PMMA-1s	MMA	2.0	201	52	20.1
PMMA-2s	MMA	1.0	336	36	20.4
PMMA-3s	MMA	0.5	384/553	32/55	18.5
PMMA-4s	MMA	0.25	378/520	34/48	15.3

[a] In all samples the "s" refers to polymerization carried out in small batches (see the Supporting Information for further details).

Table 2. Concentration series of **Fluoro-PET** for stability test, for styrene and methyl methacrylate polymerizations.

Samples[a]	Monomer	Surf. ratio	DLS		Solid content [%]
			d_h [nm]	σ [nm]	
PS-6s	St	2.0	116	18	21.0
PS-7s	St	1.0	125	19	20.5
PS-8s	St	0.5	140	19	19.2
PS-9s	St	0.25	189	22	19.5
PMMA-6s	MMA	2.0	203	23	20.9
PMMA-7s	MMA	1.0	166	25	18.9
PMMA-8s	MMA	0.5	211	29	20.2
PMMA-9s	MMA	0.25	214	28	18.2

[a] In all samples the "s" refers to polymerization carried out in small batches (see the Supporting Information for further details).

The previous results show that **C11-PET** and **Fluoro-PET** can also be viewed as effective surfmers since they were highly efficient stabilizing the miniemulsion and the resulting dispersion. Figure 3 shows two representative images of styrene nanoparticles obtained with **C11-PET** in Figure 3 A and **Fluoro-PET** in Figure 3 B.

The covalent attachment of **C11-PET** to the polymer backbone, however, was once again difficult to study, although all the results led to the same conclusion as for **C12-PET**, thus strongly suggesting its copolymerization. It is in this context that **Fluoro-PET** was exploited to further study the copolymerization of surfmers since, besides the NMR experiments, it was also possible to perform SEC measurements by using both an RI and UV/Vis detector; the latter was set up at 440 nm corresponding to the maximal absorption of **Fluoro-PET**. The results for a **PS** and a **PMMA** system are shown in Table 3, which also shows the SEC result for pure **Fluoro-PET**.

An additional feature of the latexes obtained by copolymerization of **Fluoro-PET** is that they were fluorescent in all the cases. Although no quantification was carried out, this would strongly indicate that no complete self-quenching happened between the **Fluoro-PET** molecules, or at least it was not a dominant effect. Thus, a homogeneous distribution of the surfmer on the particle surface is assumed.

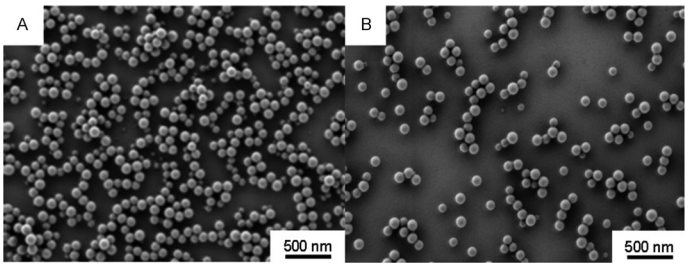

Figure 3. SEM images of polystyrene nanoparticles polymerized with **C11-PET** (A) and **Fluoro-PET** (B), corresponding to samples **PS-2s** and **PS-7s**, respectively.

Table 3. SEC results for **Fluoro-PET** polymerizations of styrene and methyl methacrylate.

Sample	M_n		M_w		PDI	
	RI	UV[a]	RI	UV[a]	RI	UV[a]
PS-7s	18×10^4	21×10^4	36×10^4	39×10^4	2.01	1.86
PMMA-7s	8.5×10^4	10×10^4	24×10^4	24×10^4	2.33	2.84
Fluoro-PET	–	474	–	553	–	1.17

[a] In all samples the UV/Vis detector was always set at 440 nm, which corresponds to the maximal absorption of Fluoro-PET.

Efficiency on the surface functionalization by using surfmers versus monomers: The quantification of the phosphonate groups on the particle surface was performed by means of a polyelectrolyte titration with the oppositely charged polyelectrolyte. A low molecular-weight polydiallyldimethylammonium chloride (polyDADMAC) was employed as polyelectrolyte. The titration endpoint was determined as the point of zero streaming potential, by using a particle charge detector (PCD, Mütek, Germany). The measurements were conducted with diluted dispersions (0.1 wt%) at pH 10.8, to ensure that all phosphonate groups are completely deprotonated in the aqueous solution ($pK_1=2.6$ and $pK_2=7.3$). The amount of functional groups were calculated from the consumed volume of polyelectrolyte, the solid content, the particle size, and the polymer density according to a reported methodology.[40] The results are summarized in Table 4 and further results are provided in the supporting information in Table S2 (see the Supporting Information).

Table 4. PCD results for the miniemulsion polymerizations carried out using the different surfmers and **SDP**.

Samples	Surf. type	d_h [nm][a]	$-PO_3^{2-}$ groups				
			Per g of polymer $\times10^{18}$	Per g of polymer $\times10^{18}$	Per g of polymer $\times10^{18}$	Max. Theo. per g of polymer $\times10^{18}$	Incorp. efficiency
PS-4	**SDP**	98	11.0	0.57	0.19	–	–
PS-5	**C12-PET**	107	27.3	1.83	0.51	50.0	54
PS-6	**C11-PET**	118	26.0	2.00	0.51	50.0	52
PS-6s	**Fluoro-PET**	124	47.5	4.96	1.03	50.0	95

[a] These values correspond to dialyzed samples.

 © 2012 Wiley-VCH Verlag GmbH & Co. KGaA, Weinheim

Table 4 shows that the use of surfmers leads to a much higher number of charges on the particle surface. Even though the samples with surfmer were much longer dialyzed than the **SDP** samples, there was no lack of dispersion stability. Moreover, **C11-PET** and **C12-PET** behaved very similarly; not only producing particles in the same size range but also introduced approximately the same amount of $-PO_3^{2-}$ groups on the surface of the particles.

We have recently reported the functionalization of nanoparticles with phosphonate groups through copolymerization of conventional monomers with either vinylphosphonic acid (VPA) or vinylbenzylphosphonic acid (VBPA).[28a] The amount of functional groups was extremely dependent on the hydrophilicity of the monomer. Whereas the functionalization density with VPA (as the more hydrophilic monomer) is rather poor, VBPA led to much higher functionalization densities. If the amount of phosphonate groups is calculated on the mass of polymer, 1% of VBPA led to almost the same functionalization density as when the same molar amount of **C12-PET** is used. In the latter case, however, much smaller particles are obtained, which may be beneficial in the suggested application for the coating of titania implant materials since the packing on surfaces would be more dense with smaller particles.

Application studies of the phosphonate-functionalized nanoparticles: As already mentioned in the introduction, phosphonic acids have a variety of applications, but only little is known about nanoparticles that are surface-functionalized with phosphonic acid groups. As the miniemulsion process would also allow the embedding of drugs and growth factors into nanoparticles, we investigated the viability and applicability of the functionalized nanoparticles as templates for the biomimetic mineralization and also performed cellular-uptake experiments to evaluate their use in biological systems.

Cellular uptake and cytotoxicity of phosphonate-functionalized nanoparticles: Several studies on the interactions between different cell types and nanoparticles presenting different sizes, shapes, and surface functionalization have been reported.[19a,41] For instance, we have highlighted how beneficial the exploitation of phosphonic acids on the particle surface is toward biological application, such as cellular uptake experiments[42] and coatings for implant materials.[18a] In those studies, the particles were obtained by the copolymerization of synthetic co-monomers using surfactants. Herein, we present preliminary results showing the successful exploitation of phosphonate-functionalized nanoparticles generated by miniemulsion polymerization under surfactant-free conditions by using the previously synthesized surfmers in cellular-uptake experiments.

Specifically, two types of human cells, a cervix cancer cell line (HeLa) and human mesenchymal stem cells (MSCs) were studied. Using both surfmers (**C12-PET** and **C11-PET**) and the conventional **SDP** surfactant (as a reference), not only the cellular uptake but also the cytotoxicity of the obtained synthesized latexes were investigated. Since the nanoparticles were dye-labeled, confocal laser scanning microscopy (CLSM) was also applied to gain better insights into the uptake. To this end, the cells were treated with 75 $\mu g\,mL^{-1}$ of fluorescent-labeled nanoparticles for 20 h and both the particle uptake and the cytotoxicity were quantified by flow cytometry. The number of dead cells (cytotoxicity) was quantified with the fluorescent DNA-intercalating dye 7-AAD, which can enter only into dead cells with disintegrated membranes.[43]

Figure 4A shows the HeLa cells uptake results obtained for phosphonate-functionalized polystyrene particles polymerized using **C12-PET** and **SDP**. The experiments were carried out with dialyzed and non-dialyzed samples of each latex. Thus, **PS-4_d** and **PS-4_nd** correspond to dialyzed and non-dialyzed nanoparticles polymerized using the conventional **SDP**, whereas **PS-5_d** and **PS-5_nd** correspond to surfmer-polymerized nanoparticle dialyzed and non-dialyzed, respectively, (for a detailed particle description see Table S1 in the Supporting Information).

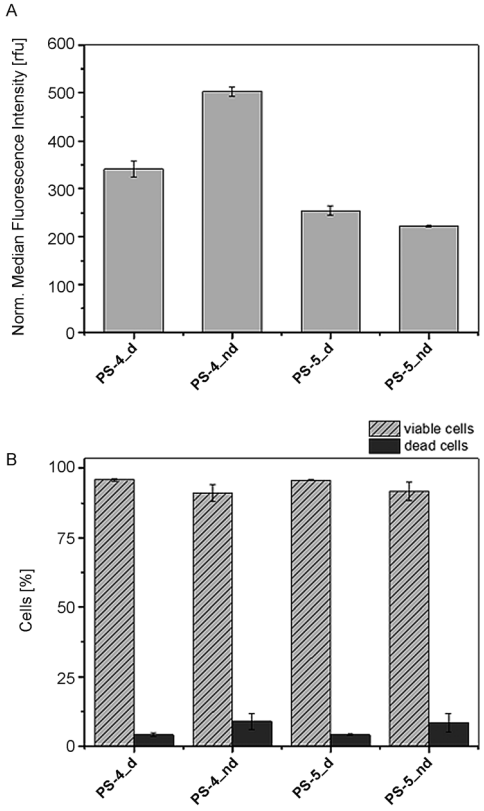

Figure 4. Uptake and viability of phosphonate-functionalized nanoparticles: **PS-4_d** and **PS-4_nd** corresponding to dialyzed and non-dialyzed nanoparticles polymerized using the conventional **SDP**, and **PS-5_d** and **PS-5_nd** corresponding to surfmer-polymerized nanoparticle dialyzed and non-dialyzed. HeLa cells were incubated with 75 $\mu g\,mL^{-1}$ fluorescently (PMI) labeled nanoparticles for 20 h and both particle uptake (A) and cytotoxicity (B) were analyzed by flow cytometry. Particle cell uptake was normalized to the fluorescence value of a standard polystyrene nanoparticle and expressed as normalized median fluorescence intensity (rfu; relative fluorescence units). Mean values and standard deviations were calculated from two independent experiments which were run in triplicate.

 © 2012 Wiley-VCH Verlag GmbH & Co. KGaA, Weinheim

Phosphonate-functionalized nanoparticles showed similar uptake rates in HeLa cells for the analyzed samples with exemption of the non-dialyzed **SDP** stabilized particles **PS-4_nd**, which experienced about 30% higher uptake ratio than its corresponding dialyzed **PS-4_d**. It is worth noting that although a higher surfactant (**SDP**) concentration seems to favor the cellular uptake, the result clearly evidences a strong dependence on the purification level (see the Experimental Section). This inconvenience is not observed in the surfmer-polymerized samples, in which the cell uptake ratios were similar regardless of the dialysis of the samples.

Figure 4B shows the results for the viability analysis measured by flow cytometry for the aforementioned samples, namely **PS-4_d**, **PS-4_nd**, **PS-5_d**, and **PS-5_nd**. It can be seen from this Figure that whereas the dialyzed nanoparticles presented a negligible cytotoxicity ($\approx$5% apoptotic cells), the non-dialyzed samples exhibited a very small toxic effect ($\approx$10% apoptotic cells). These results were independent on the use of **C12-PET** or **SDP**.

The human MSCs showed uptake rates of approximately one order of magnitude lower than HeLa cells for the same set of studied samples (see the Supporting Information, Figure S1).

The exploitation of **C11-PET** as surfmer was also investigated for these cell-uptake experiments showing no differences when compared to the results obtained for **C12-PET** (see the Supporting Information).

Finally, Figure 5 shows confocal live-cell images of HeLa cells after the uptake of different nanoparticles (which appear as green in the images due to dye used to label them). Figure 5A shows the uptake results using **PS-5_d**, whereas Figure 5B shows the results obtained for **PS-6_d** (which was synthesized using **C11-PET**, see Table S1 in the Supporting Information). Additional and comprehensive CLSM images of the uptake experiments with different surfmer-functionalized and **SDP**-stabilized particles in HeLa and human MSCs are shown in Figure S2 in the Supporting Information.

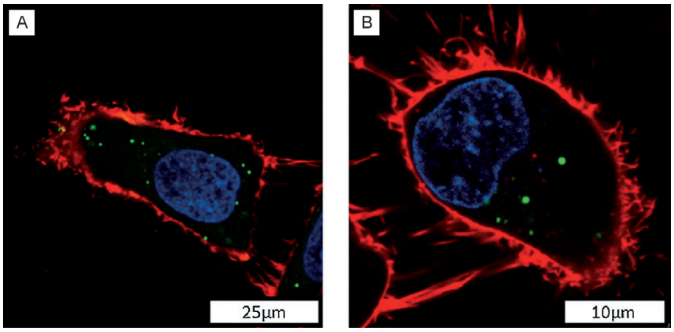

Figure 5. Confocal live cell images of HeLa cells incubated with 75 $\mu g\,mL^{-1}$ of latexes **PS-5_d** (A) and **PS-6_d** (B) for 20 h. The cell membrane was stained with CellMask Orange (appears red), the nucleus was stained with DraQ5 (appears blue), and the particles were labeled with PMI (appears green).

These results are in accordance with other studies, in which phosphonate-functionalized particles showed a good uptake in dendritic[44] and mesenchymal stem cells[5] without a significant damage on the viability. Phosphonate-functionalized particles also do not impair cell proliferation and activity.[5,45]

Apatite growth on the particle surface of phosphonate-functionalized nanoparticles: We have previously reported that phosphonate-functionalized particles of about 200 nm were successfully mineralized in dispersion or adhered to a titanium substrate[18] It was found that it was critical to synthesize smaller surface-functionalized nanoparticles without using large amounts of non-ionic surfactant nor SDS as surfactant, which showed to counteract an effective loading with minerals,[2] resulting in only very small amounts of hydroxyapatite (HAP) crystals on the particle surface. The low amount of crystals found on the particle surface was explained by a possible shielding effect of the functional groups by excess of non-ionic surfactant or small residues of SDS that could not be removed from the particle surface in the washing step.[2] Herein, we have demonstrated that by using a surfmer for the synthesis of small functionalized particles these problems were circumvented. Phosphonate-functionalized particles of around 100 nm size were synthesized through a surfmer-approach and applied to grow HAP on the particle surface. The morphology of the untreated particles were already shown in Figure 3A.

Mineralization onto the surface of the functionalized particles was carried out following an already reported methodology,[18b] basically consisting on the sequential loading of the surface with the respective ions. Once the process was finished, the particles were homogeneously covered with crystals as it can be seen in the SEM overview image (Figure 6A). In the enlarged TEM image (Figure 6B) numerous

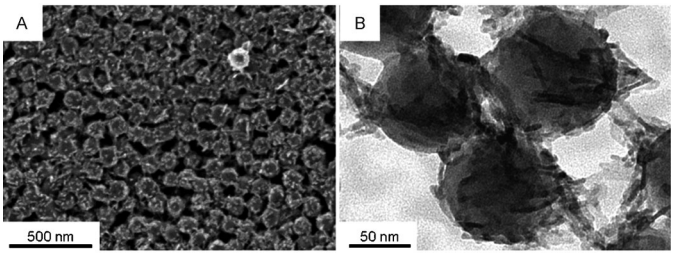

Figure 6. SEM (A) and TEM (B) images showing the formation of HAP crystals on the surface of phosphonate-functionalized nanoparticles prepared with **C11-PET**.

crystals attached to the particles are clearly visible. To maintain the colloidal stability of the dispersion during the crystallization process, very small amounts of a nonionic surfactant (Lutensol AT50) were added before the loading. XRD revealed that the crystals formed on the surface of the particles are indeed hydroxyapatite (see the Supporting Information, Figure S3). The crystalline nature of the HPA was additionally confirmed by using dark field TEM images (shown

 © 2012 Wiley-VCH Verlag GmbH & Co. KGaA, Weinheim

in the Supporting Information, Figure S4). The thermogravimetric analysis of the sample showed that the percentage of inorganic material in the sample is 32.9%, which is in accord with the theoretical value of 33.3% (see the Supporting Information, Figure S5).

Conclusion

In this paper we described the synthesis of three new surfmers for miniemulsion polymerizations and employed them in the polymerization of different monomers. All surfmers were successfully copolymerized, without using any additional surfactants and generating very stable dispersions (even after several months of storage), with a narrow particle size distribution. One of the synthesized surfmers (**Fluoro-PET**) bears a fluorescent label and is the first dye-labeled surfmer. The use of this **Fluoro-PET** permitted us to study and evaluate the copolymerization between the surfmer and the other monomers by studying the resulting polymers by using SEC with both the RI and the UV-detector (set up at 440 nm corresponding to the maximal absorption of **Fluoro-PET**) simultaneously. The excellent agreement between the UV and RI chromatograms of the polymer-forming particle confirmed the successful copolymerization. This is a new approach that contributes to the long discussed field of copolymerization of surfmers.

Regarding the application studies of these phosphonate-functionalized nanoparticles, two preliminaries studies were carried out: cell uptake of the functionalized nanoparticles and biomimetic mineralization of hydroxyapatite on their surface. On one hand, the favorable affinity of phosphonate groups on the surface of the nanoparticles toward two different cell types, a cervix cancer line (HeLa) and a human mesenchymal stem cell (MSC), was exploited to study their uptake without significant cytotoxicity. Thus, we demonstrated here that surfmers provide a new area for the development of new functionalized nanoparticles, which can be obtained by miniemulsion polymerization with good intracellular uptakes rates for drug release in target cells, or for developing tailored surfmers toward metal prostheses with good biocompatibility. On the other hand, the same phosphonate-functionalized nanoparticles were used as functional scaffolds allowing the binding of calcium ions to subsequently mineralize hydroxyapatite on the surface of the particles. The results showed a high density of crystal grown on the particle surface due to the high and uniform decoration of the surface with phosphonic acid groups, which was provided by the copolymerization of the surfmers.

It is worth mentioning that the herein-described surfmer approach can effectively and controllably produce smaller particles than the conventional approach using co-monomers, and has no need for additional surfactants that might cause difficulties in further envisaged applications.

Finally, we expect this functional surfmer approach, including their potential applicability in the different research areas, to greatly contribute to the field of functional nanoparticles, from their design, synthesis and functionalization, to their final applications.

Experimental Section

Synthesis of the surfmers and miniemulsion polymerizations: The entire synthesis and characterization of each surfmer, as well as all miniemulsion polymerizations are fully described in the Supporting Information.

Methods: ^{1}H, ^{13}C, and ^{31}P spectra were recorded on Bruker Avance spectrometers with 250, 300, or 500 MHz. For ^{1}H- and ^{13}C NMR spectra tetramethylsilane was used as an external standard. In the case of ^{31}P NMR spectra, triphenylphosphine was employed as an external reference; the signal of triphenylphosphine was set at $\delta = -6.0$ ppm.

Purification and characterization of the functionalized polymer nanoparticles: All latexes were purified by dialysis. To evaluate the efficiency of the purification, samples were measured at different dialysis time. As a result, latexes were dialyzed for at least six days, with a daily water change.

Surface tension was determined by the DuNoüy ring method at 20°C with a DCAT 21 device (Dataphysics, Filderstadt, Germany). All values presented were averaged over ten repetitions of push–pull cycles. The average hydrodynamic diameter D_H of the particles and the particle size distribution were measured by dynamic light scattering (DLS) (photon cross-correlation spectroscopy PCCS) using a Nanophox PCCS (Sympatec GmbH, Clausthal-Zellerfeld, Germany) at an scattering angle of 90° and a temperature of 25°C. Dispersions were diluted to approximately 0.1 wt% with distilled water. The measurement parameters were set to a count rate of 200 kcps with a measuring time of 100 s for each run and three repetitions were conducted. The raw data was plotted in origin and a gauss fit was done. Scanning electron microscopy (SEM) images were taken with a Gemini 1530 (Carl Zeiss AG, Oberkochen, Germany). The samples were prepared by drop casting of 0.01 wt.% dispersions on silicon wafers. The density of the functional groups on the particle surface was determined by titration against the oppositely charged polyelectrolyte poly(diallyldimethyl ammonium chloride) (PDADMAC) using a particle charge detector (Mütek GmbH, Germany) in combination with a Titrino Automatic Titrator (Metrohm AG, Switzerland). The measurements were conducted on 10 mL of the latex sample with a solid content of 1 mg mL^{-1}. The number of groups was calculated from the polyelectrolyte consumption according to a methodology already reported.[40]

Mineralization of phosphonate-functionalized particles: The loading of the particles was performed at 37°C under stirring. The stability of the particle dispersion was provided by adding 0.8 wt% nonionic surfactant Lutensol AT50-containing aqueous solution by multiple centrifugation and redispersion. First, the pH of all solutions was adjusted with a 28% ammonia solution. Then, $Ca(NO_3)_2$ (0.5 mmol) was added to polymer particles ($\approx$0.1 g) and stirred for 2 h to allow the binding of calcium ions to the particle surface. Afterwards an aqueous solution of $(NH_4)_2HPO_4$ (0.3 mmol) was added drop-wise during 1 h. After the loading process, the samples were stirred for about 24 h. All the loadings were performed at a constant molar ratio of calcium to phosphate ions of 5:3. The pH of the particle dispersion was kept constant at pH 10 during the whole loading experiment. The loaded samples were washed and freeze-dried before XRD and TGA measurements. X-ray diffraction (XRD) was carried out with a Phillips Typ PW diffractometer with Cu-Kα radiation (λ = 1.54 Å), 40 kV voltage, and 30 mA current.

Cellular uptake and cytotoxicity: *Cell culture*: Human cervix carcinoma cells (HeLa) were kept in Dulbecco's modified eagle medium (DMEM), supplemented with FCS (10%), penicillin (100 units) and streptomycin (100 mg mL^{-1}), and L-glutamine (2×10^{-3} M) (all from Invitrogen, Germany). Cells were grown in a humidified incubator at 37°C and 5% CO_2.

For the nanoparticle uptake and the cytotoxicity measurements, adherent HeLa cells were seeded at a density of 15,000 cells cm^{-2} in 6-well-plates (Greiner, Germany). On the following day, fluorescent particles (labeled with PMI) were added at a concentration of 75 μg mL^{-1} to the media in

 © 2012 Wiley-VCH Verlag GmbH & Co. KGaA, Weinheim

the 6-well-plates without using a transfection agent. On the third day, adherent cells in the 6-well-plates were detached in 2.5% trypsin (Gibco, Germany), washed with magnesium- and calcium-free phosphate buffered saline (PBS, Gibco, Germany), incubated with 7-aminoactinomycin (7-AAD, 28.6 $\mu g\,mL^{-1}$) for 15 min at room temperature for the analysis of cell viability and centrifuged. The pellet was resuspended in PBS for analysis by flow cytometry.

For the dilution series of the surfactants SDS and **SDP**, 30,000 cells cm^{-2} HeLa cells were seeded in 96-well-plates (Corning, USA). The surfactants were solved in H_2O and serial dilutions in DMEM with FCS (10%) were performed. After 24 h, the cells were treated with the indicated surfactant concentrations and incubated for 20 h in a humidified incubator (37 °C, 5% CO_2). The live/dead staining were directly performed in the 96-well-plates with a final concentration of 1 μM calcein-AM (Invitrogen) and propidium iodide (40 $\mu g\,mL^{-1}$; Fluka, Germany) for 30 min at room temperature in the dark. Subsequently, the fluorescently stained cells were measured with a fluorescence plate reader (Infinite M1000, Tecan, Germany), excited with 490 nm, and detected at 530 nm for calcein, and excited with 530 nm and detected at 645 nm for propidium iodide, using i-control software (Tecan, Germany).

Flow cytometry analysis: For the analysis of cell viability and the quantification of cellular uptake of the nanoparticles, flow cytometry was used. Flow cytometry measurements were performed with a CyFlow ML using FlowMax 2.57 software (Partec, Germany). The FL1 channel (527 nm) was used to analyze the uptake of nanoparticles, which were excited with 488 nm, and FL6 (675 nm) was used for 7-AAD measurements, which were excited with 561 nm. For analysis, cells were selected on a forward scatter/sideward scatter plot, thereby excluding cell debris. These gated events were further analyzed for the FL1 and FL6 channels. The median in FL1 was determined by analysis of 1D histograms. This demonstrates the amount of nanoparticles taken up or associated with individual cells. For 7-AAD, the events in the cell gate were analyzed on a FL1/FL6 dot-plot and three different populations (viable, apoptotic, or dead) were determined by using negative controls and the apoptotic and dead cells present in cell cultures. All values are triplicates of two independent experiments with standard deviation. To normalize the median fluorescence values from the flow cytometry measurement and to compare the values of all particles it is necessary to introduce the factor of particle fluorescence intensity (FLI_{PR-Px}). For the normalization process particle fluorescence intensity (FLI_{PR-Px}) was measured at a concentration of 75 $mg\,mL^{-1}$ in PBS in black 96-well-plates with clear bottoms (Corning, USA). Measurements were performed with a plate reader Infinite M1000 (Tecan, Germany), excited with 488 nm (±5 nm), and detected at 527 nm (±5 nm) by using i-control software (Tecan, Germany). The fluorescence intensity (FLI_{PR-Px}) of 75 $mg\,mL^{-1}$ particles measured by the plate reader was first normalized on the fluorescence intensity of 75 $mg\,mL^{-1}$ nonfunctionalized polystyrol particle expressed as normalized fluorescence intensity (nFL_{PR} [Eq. (1)]). Then the median fluorescence intensity of the particle Px ($MFLI_{FACS-Px}$) measured by flow cytometry was normalized to nFL_{PR} [Eq. (2)]:

$$nFL_{PR} = FLI_{PR-Px}/FLI_{PR-PS} \quad (1)$$

$$nMFL_{Px} = MFLI_{FACS-Px}/nFL_{PR} \quad (2)$$

in which FLI_{PR-Px} is the fluorescence intensity of particle x (plate reader); FLI_{PR-PS} is the fluorescence intensity of nonfunctionalized polystyrol particle (plate reader); nFL_{PR} is the normalized fluorescence intensity (plate reader); $MFLI_{FACS-Px}$ is the median fluorescence intensity of particle x (flow cytometry), and $nMFL_{Px}$ is the normalized median fluorescence intensity of particle x

Confocal laser scanning microscopy (CLSM): CLSM was performed to demonstrate the intracellular localization of the different particles. For the confocal laser scanning microscopy the HeLa cells were seeded in FCS-supplemented DMEM at a density of 10,000 cells cm^{-2} in ibiTreat μ-slides (IBIDI, Germany). On the second day, particles were added to FCS-supplemented medium at a concentration of 75 $\mu g\,mL^{-1}$ without transfection agent. Before CLSM imaging cells were washed two times with PBS. Images were taken with a commercial setup (LSM SP5 STED Leica Laser Scanning Confocal Microscope, Leica, Germany), consisting of inverse fluorescence microscope DMI 6000 CS equipped with a multi-laser combination and with five detectors operating in the range of 400–800 nm. A HCX PL APO CS 63×1.4 oil objective was used for these studies. The fluorescent particles were excited with the argon laser ($\approx$5 mW, λ = 488 nm), detected at 510–550 nm and are pseudo-colored in green. Cell membrane was stained with CellMask Orange (2.5 $mg\,mL^{-1}$, Invitrogen, Germany), excited with DPSS 561 nm ($\approx$20 mW), detected at 580–620 nm. This signal from the cell membrane was pseudo-colored in red surrounding the cytoplasm. The cell nucleus was stained with DraQ5 (2.5×10^{-6} M, Biostatus, UK), excited with HeNe-laser (633 nm, $\approx$10 mW), detected at 680–750 nm and appears in blue.

Acknowledgements

We thank Gunnar Glaser for support with the electron microscopy, and Hansjörg Menges for fluorescence measurements and studies.

[1] K. Landfester, *Angew. Chem.* **2009**, *121*, 4556; *Angew. Chem. Int. Ed.* **2009**, *48*, 4488.
[2] A. Ethirajan, U. Ziener, K. Landfester, *Chem. Mater.* **2009**, *21*, 2218.
[3] a) M. Y. Hua, H. W. Yang, H. L. Liu, R. Y. Tsai, S. T. Pang, K. L. Chuang, Y. S. Chang, T. L. Hwang, Y. H. Chang, H. C. Chuang, C. K. Chuang, *Biomaterials* **2011**, *32*, 8999; b) R. N. Grass, E. K. Athanassiou, W. J. Stark, *Angew. Chem. Int. Ed.* **2007**, *46*, 4909.
[4] W. J. Stark, *Angew. Chem. Int. Ed.* **2011**, *50*, 1242.
[5] A. Tautzenberger, S. Lorenz, L. Kreja, A. Zeller, A. Musyanovych, H. Schrezenmeier, K. Landfester, V. Mailänder, A. Ignatius, *Biomaterials, 31*, 2064.
[6] D. Shi, M. Matsusaki, M. Akashi, *J. Controlled Release* **2011**, *149*, 182.
[7] a) C. Cardenas-Daw, A. Kroeger, W. Schaertl, P. Froimowicz, K. Landfester, *Macromol. Chem. Phys.* **2012**, *213*, 144; b) P. Froimowicz, H. Frey, K. Landfester, *Macromol. Rapid Commun.* **2011**, *32*, 468.
[8] a) M. Antonietti, K. Landfester, *Prog. Polym. Sci.* **2002**, *27*, 689; b) F. J. Schork, W. Smulders, J. P. Russum, A. Butté, K. Fontenot, *Adv. Polym. Sci.* **2005**, *175*, 129.
[9] R. G. Gilbert, *Emulsion Polymerization: A Mechanistic Approach*, Academic: San Diego, **1995**.
[10] M. Okubo, M. Nomura, H. Tobita, K. Suzuki, in *Polymer Particles, Vol. 175*, Springer Berlin/Heidelberg, **2005**, pp. 1.
[11] K. Landfester, *Macromol. Rapid Commun.* **2001**, *22*, 896.
[12] W. Li, K. Min, K. Matyjaszewski, F. o. Stoffelbach, B. Charleux, *Macromolecules* **2008**, *41*, 6387.
[13] H. Matahwa, J. B. Mcleary, R. D. Sanderson, *J. Polym. Sci. A: Polym. Chem.* **2006**, *44*, 427.
[14] A. Guyot, *Adv. Colloid Interface Sci.* **2004**, *108–109*, 3.
[15] E. T. W. M. Schipper, O. Sindt, T. Hamaide, P. Lacroix-Desmazes, B. Müller, A. Guyot, M. J. W. A. van den Enden, F. Vidal, J. J. G. S. van Es, A. L. German, A. Montaya Goñi, D. C. Sherrington, H. A. S. Schoonbrood, J. M. Asua, M. Sjöberg, *Colloid Polym. Sci.* **1998**, *276*, 402.
[16] A. Guyot, *Macromol. Symp.* **2002**, *179*, 105.
[17] J. Asua, H. Schoonbrood, *Acta Polym.* **1998**, *49*, 671.
[18] a) A. Zeller, A. Musyanovych, M. Kappl, A. Ethirajan, M. Dass, D. Markova, M. Klapper, K. Landfester, *ACS Appl. Mater. Interfaces* **2010**, *2*, 2421; b) K. Schöller, A. Ethirajan, A. Zeller, K. Landfester, *Macromol. Chem. Phys.* **2011**, *212*, 1165.
[19] a) V. Holzapfel, A. Musyanovych, K. Landfester, M. R. Lorenz, V. Mailänder, *Macromol. Chem. Phys.* **2005**, *206*, 2440; b) E. M. Coen, R. A. Lyons, R. G. Gilbert, *Macromolecules* **1996**, *29*, 5128.
[20] D. Crespy, A. Musyanovych, K. Landfester, *Colloids Polymer Sci.* **2006**, *284*, 780.
[21] J. L. Guillaume, C. Pichot, J. Guillot, *J. Polymer Sci. Polymer Chem., 28*, 137.

 © 2012 Wiley-VCH Verlag GmbH & Co. KGaA, Weinheim

[22] M. Herold, H. Brunner, G. E. M. Tovar, *Macromol. Symp. Macromolecular Chemistry and Physics* **2003**, *204*, 770.
[23] M. J. Unzué, H. A. S. Schoonbrood, J. M. Asua, A. M. Goñi, D. C. Sherrington, K. Stähler, K. H. Goebel, K. Tauer, M. Sjöberg, K. Holmberg, *J. Appl. Polym. Sci.* **1997**, *66*, 1803.
[24] D. Francová, G. Kickelbick, *Macromol. Chem. Phys.* **2009**, *210*, 2037.
[25] D. Francová, G. Kickelbick, *Monatsh. Chem.* **2009**, *140*, 413.
[26] N. Moszner, J. Pavlinec, I. Lamparth, F. Zeuner, J. Angermann, *Macromol. Rapid Commun.* **2006**, *27*, 1115.
[27] G. Titvinidze, A. Kaltbeitzel, A. Manhart, W. H. Meyer, *Fuel Cells, 10*, 390.
[28] A. Ziegler, K. Landfester, A. Musyanovych, *Colloid Polym. Sci.* **2009**, *287*, 1261.
[29] R. G. G. Russell, M. J. Rogers, *Bone* **1999**, *25*, 97.
[30] a) A. C. Herranz, L. J. Costa, C. F. J. Domingo, *Afinidad* **1985**, *42*, 82; b) V. Verdinelli, B. Vuano, P. C. Schulz, P. V. Messina, *J. Disper. Sci.Technol.* **2009**, *30*, 1538.
[31] A. Guyot, *Microspheres Microcapsules Liposomes* (Eds.: R. Arshady, A. Guyot), Citus Books, London, **2002**, p. 77.
[32] H. R. Ing, R. H. F. Manske, *J. chem. soc.* **1926**, *129*, 2348.
[33] N. H. C. C. E. Mc Kenna. M. T. Higa, M. C. Mc Kenna, *Tetrahedron Lett.* **1977**, *18*, 155.
[34] a) F. Boisson, I. Uzulina, A. Guyot, *Macromol. Rapid Commun.* **2001**, *22*, 1135; b) Y. Zheng, Y. Cao, G. Pan, *Ultrason. Sonochem.* **2008**, *15*, 314.
[35] K. Takahashi, K. Nagai, *Polymer* **1996**, *37*, 1257.
[36] H. A. S. Schoonbrood, J. M. Asua, *Macromolecules* **1997**, *30*, 6034.
[37] A. Pich, S. Datta, A. Musyanovych, H.-J. P. Adler, L. Engelbrecht, *Polymer* **2005**, *46*, 1323.
[38] a) N. Felorzabihi, P. Froimowicz, J. C. Haley, G. R. Bardajee, B. Li, E. Bovero, F. C. J. A. van Veggel, M. A. Winnik, *J. Phys. Chem. B* **2009**, *113*, 2262; b) P. Froimowicz, D. Klinger, K. Landfester, *Chem. Eur. J.* **2011**, n/a.
[39] F. Garwe, A. Schonhals, H. Lockwenz, M. Beiner, K. Schroter, E. Donth, *Macromolecules* **1996**, *29*, 247.
[40] A. Musyanovych, R. Rossmanith, C. Tontsch, K. Landfester, *Langmuir* **2007**, *23*, 5367.
[41] a) S. E. A. Gratton, P. A. Ropp, P. D. Pohlhaus, J. C. Luft, V. J. Madden, M. E. Napier, J. M. DeSimone, *Proc. Natl. Acad. Sci. USA* **2008**, *105*, 11613; b) J. Dausend, A. Musyanovych, M. Dass, P. Walther, H. Schrezenmeier, K. Landfester, V. Mailänder, *Macromol. Biosci.* **2008**, *8*, 1135; c) A. Villanueva, M. Cãete, A. G. Roca, M. Calero, S. Veintemillas-Verdaguer, C. J. Serna, M. Del Puerto Morales, R. Miranda, *Nanotechnology* **2009**, *20*; d) G. Baier, C. Costa, A. Zeller, D. Baumann, C. Sayer, P. H. H. Araujo, V. Mailänder, A. Musyanovych, K. Landfester, *Macromol. Biosci.* **2011**, *11*, 628.
[42] A. Tautzenberger, L. Kreja, A. Zeller, S. Lorenz, H. Schrezenmeier, V. Mailänder, K. Landfester, A. Ignatius, *Biomaterials* **2011**, *32*, 1706.
[43] D. Wlodkowic, J. Skommer, D. McGuinness, S. Faley, W. Kolch, Z. Darzynkiewicz, J. M. Cooper, *Anal. Chem.* **2009**, *81*, 6952.
[44] A. M. Mumin, J. W. Barrett, G. A. Dekaban, J. Zhang, *J. Colloid Interface Sci.* **2011**, *353*, 156.
[45] A. Tautzenberger, L. Kreja, S. Lorenz, A. Zeller, H. Schrezenmeier, V. Mailänder, K. Landfester, A. Ignatius, *Bone* **2011**, *48*, *Supp. 2*, S125.

Received: October 15, 2011
Published online: March 29, 2012

 © 2012 Wiley-VCH Verlag GmbH & Co. KGaA, Weinheim